Effect of Uncertainty in Water Vapor Continuum Absorption on Radiative Forcing, Longwave Feedback, and Climate Sensitivity

Florian E. Roemer[1,2], Stefan A. Buehler[1], Lukas Kluft[3], and Robert Pincus[4]

[1]Center for Earth System Research and Sustainability (CEN), Meteorological Institute, Universität Hamburg, Hamburg, Germany

[2]International Max Planck Research School on Earth System Modelling (IMPRS-ESM), Hamburg, Germany

[3]Max Planck Institute for Meteorology, Hamburg, Germany

[4]Lamont-Doherty Earth Observatory, Columbia University, Palisades, New York, USA

Key Points:

- Water vapor continuum absorption of terrestrial radiation is still uncertain
- Stronger continuum weakens both $2\times CO_2$ radiative forcing and longwave feedback, net increasing climate sensitivity
- Continuum uncertainty non-negligible for constraining longwave clear-sky climate sensitivity

Corresponding author: Florian E. Roemer, `florian.roemer@uni-hamburg.de`

Abstract

We assess the effect of uncertainty in water vapor continuum absorption on radiative forcing $\mathcal{F}$, longwave feedback λ, and climate sensitivity $\mathcal{S}$ at surface temperatures T_s between 270 K and 330 K. We calculate this uncertainty using a line-by-line radiative-transfer model, assuming moist-adiabatic temperature profiles, 80 % relative humidity, and spectrally uniform variations in continuum absorption of ±10 %. At $T_\mathrm{s} = 288\,\mathrm{K}$ this uncertainty translates to uncertainties of $\pm 0.02\,\mathrm{W\,m^{-2}}$ (±0.5 %) in $\mathcal{F}$ and $\pm 0.04\,\mathrm{W\,m^{-2}\,K^{-1}}$ (±2.5 %) in λ, respectively. Both $\mathcal{F}$ and λ weaken for a stronger continuum, inducing opposite effects on $\mathcal{S}$. The weaker λ dominates, causing $\mathcal{S}$ to increase by 0.05 K (2 %) for a stronger continuum at $T_\mathrm{s} = 288\,\mathrm{K}$. Overall, the effect of uncertainty in water vapor continuum absorption on $\mathcal{F}$, λ and $\mathcal{S}$ is small compared to the major sources of uncertainty but of comparable magnitude to other uncertainties affecting the relatively well-constrained longwave clear-sky $\mathcal{S}$.

Plain Language Summary

Water vapor in Earth's atmosphere acts as a strong greenhouse gas by absorbing thermal radiation and thus plays a central role in controlling Earth's climate. Although water vapor absorption is well-understood in general, some uncertainties remain in the water vapor continuum, an absorption component that is still estimated based on measurements. We investigate the impact of this uncertainty on a very simple climate model by varying the strength of continuum absorption by ±10 %. We find that if the continuum is 10 % stronger than the current estimate, a doubling of the atmospheric CO_2 concentration has a 0.5 % weaker effect on Earth's energy budget. However, Earth's ability to emit more thermal radiation to space as it warms is reduced by about 2.5 %. Overall, the temperature increase caused by a CO_2 doubling is about 0.05 K (2 %) larger if continuum absorption is 10 % stronger, and vice versa. This uncertainty caused by the continuum is small compared to the main uncertainties in the climate system, such as clouds. However, it is of comparable magnitude to other uncertainties that affect thermal radiation under clear skies.

1 Introduction

Due to its absorption of infrared radiation, water vapor plays a central role in determining Earth's energy budget. Absorption by water vapor is well-understood over-

all, but there is still uncertainty regarding the impact of line far wings and absorption by the water dimer, the effects of which are subsumed in the water vapor continuum (Shine et al., 2012). We assess the effect of this uncertainty in water vapor continuum absorption on $2 \times CO_2$ radiative forcing $\mathcal{F}$, longwave feedback λ, and climate sensitivity $\mathcal{S}$.

Uncertainty in the water vapor continuum arises because its absorption cannot be calculated from first principles. Rather, the continuum is usually estimated semi-empirically by splitting it into the foreign and self continuum which depend linearly and quadratically on water vapor concentration, respectively. Although somewhat arbitrary, this continuum definition and decomposition is well-established (e.g., Clough et al., 1989; Tipping & Ma, 1995; Mlawer et al., 2012; Shine et al., 2012). Models of continuum absorption, such as the MT_CKD model (Mlawer et al., 2012), rely on data from laboratory measurements, satellite observations, and field campaigns for their fits (e.g., Burch, 1982; Paynter et al., 2009; Odintsova et al., 2022). However, those measurements still exhibit substantial spread (Baranov et al., 2008; Shine et al., 2016; Ptashnik et al., 2011).

Continuum absorption is strongest within the water vapor absorption bands but its climate impact is strongest in the atmospheric windows where it is often the dominant absorber (Fig. 1a). The largest uncertainties in the continuum remain in the near-infrared and visible spectral ranges which affect the absorption of solar radiation (Shine et al., 2016). In this study, however, we focus on the effect of the continuum on terrestrial radiation. In this context, the mid-infrared window ($750\,\mathrm{cm}^{-1}$ to $1250\,\mathrm{cm}^{-1}$) is particularly relevant because a substantial part of the outgoing longwave radiation $\mathcal{L}$ is emitted here. At surface temperatures of around 300 K continuum absorption becomes optically thick which closes this window and strongly inhibits Earth's ability to radiate energy to space. At the same time, the spread in estimates of continuum absorption in this spectral region is still around 10–20 % and does not seem to decrease over time (see Fig. 1b, also e.g., Baranov et al., 2008; Shine et al., 2016). This raises the question as to how large the resulting uncertainty in $\mathcal{S}$ is and what this uncertainty implies for previous studies about the temperature dependence of $\mathcal{S}$ (e.g., Kluft et al., 2021; Seeley & Jeevanjee, 2021; Meraner et al., 2013; Romps, 2020).

To date, most discussions about uncertainty in water vapor continuum absorption are limited to the field of spectroscopy (e.g., Shine et al., 2012; Baranov et al., 2008; Shine et al., 2016; Ptashnik et al., 2011). Some studies investigate the effect of uncertainty in

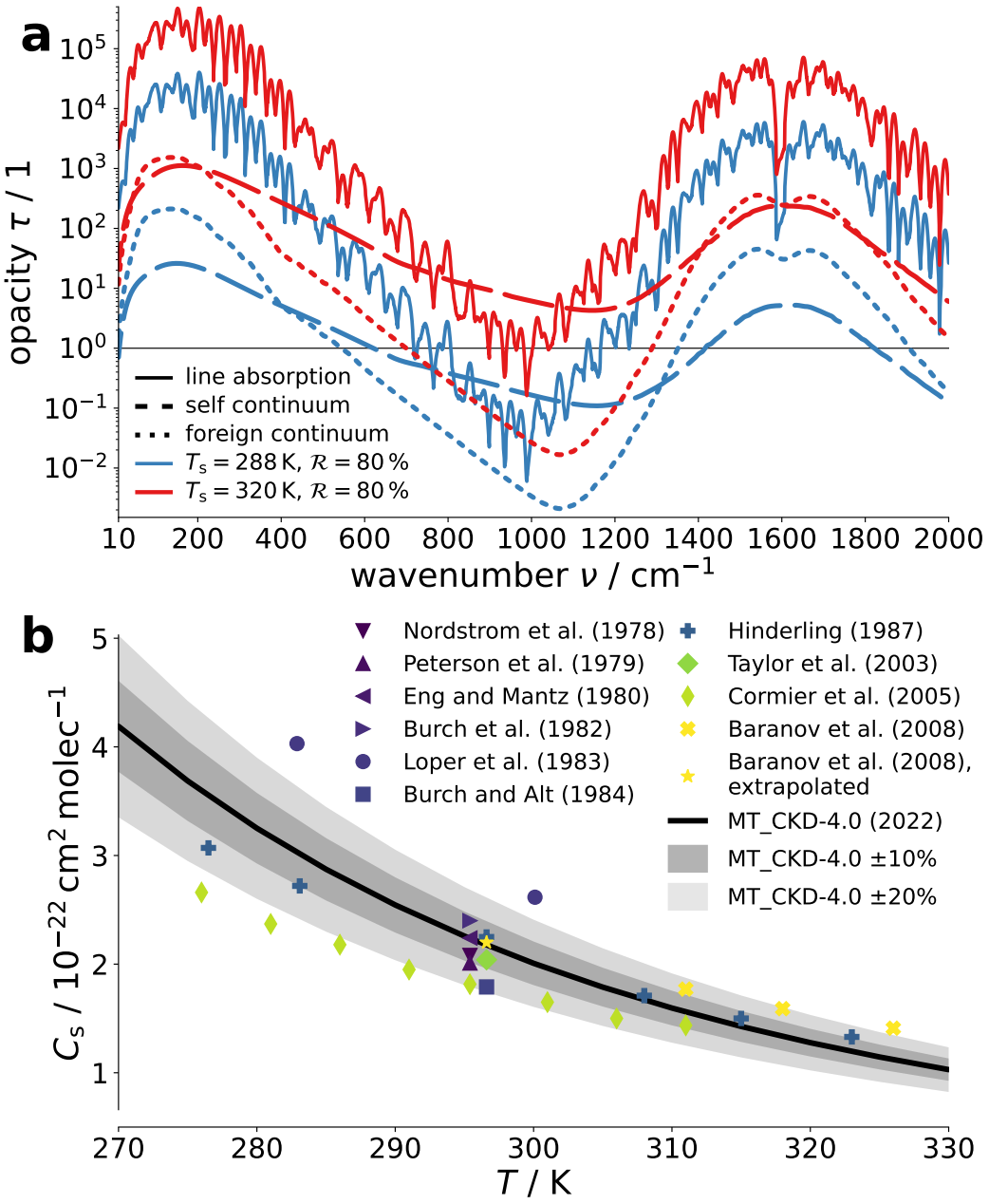

Figure 1. (a) Opacity τ of atmospheric column (80 % relative humidity) due to absorption by water vapor lines (solid), water vapor self continuum (dashed) and water vapor foreign continuum (dotted) for surface temperatures T_s = 288 K (blue) and T_s = 320 K (red). (b) Self continuum absorption cross-section C_s at 944.19 cm^{-1} as function of temperature T from MT_CKD version 4.0 (Mlawer et al., 2012) (line) and from laboratory measurements (symbols). The shaded areas correspond to differences of ±10 % and ±20 % from MT_CKD, respectively. The measurements at 296 K are slightly offset along the temperature axis for better visibility. Laboratory data were read off from Baranov et al. (2008, their Fig. 8) and Ptashnik et al. (2011, their Fig. 7).

the continuum on $\mathcal{L}$ (Paynter & Ramaswamy, 2011, 2012), while others touch on the effect of the continuum on the longwave feedback but do not discuss its uncertainty (Seeley & Jeevanjee, 2021; Koll et al., 2023; Stevens & Kluft, 2023). To expand on those studies, we take a holistic look at the effect of uncertainty in water vapor continuum absorption on $2 \times CO_2$ radiative forcing $\mathcal{F}$, longwave feedback λ, and climate sensitivity $\mathcal{S}$.

2 Methods

2.1 Model configuration

We use the radiative-convective equilibrium model konrad (Kluft et al., 2019; Dacie et al., 2019). We create profiles of temperature $\boldsymbol{T}$ and water vapor volume mixing ratio $\boldsymbol{q}$ on 512 vertical levels at a given surface temperature T_s. The $\boldsymbol{T}$ profile follows a moist adiabat in the troposphere until it reaches 175 K. Above, we assume a fixed isothermal stratosphere with $\boldsymbol{T} = 175\,\mathrm{K}$. This approach eliminates stratospheric feedbacks and allows us to focus exclusively on the troposphere. Relative humidity is set to 80 % in the troposphere and stratospheric $\boldsymbol{q}$ is set to the tropopause value. Unless stated otherwise, the CO_2 concentration is set to 348 ppm. This setup was already used and described by Kluft et al. (2021).

We perform experiments at $T_\mathrm{s} \in [269\,\mathrm{K}, 331\,\mathrm{K}]$ in 1 K increments. For each T_s we calculate the spectrum of outgoing longwave radiation $\mathcal{L}_\nu$ using the line-by-line radiative transfer model ARTS (Eriksson et al., 2011; Buehler et al., 2018). We perform the calculations at 32,768 frequencies uniformly spanning the spectral range $10\,\mathrm{cm}^{-1}$ to $3{,}250\,\mathrm{cm}^{-1}$. In the spirit of our idealized model setup (and consistent with Kluft et al., 2021), we only consider absorption by water vapor and CO_2, as well as by N_2 and O_2 due to their abundance and well-mixed nature. We do not consider the effects of other greenhouse gases such as CH_4 and O_3 which are expected to be of secondary importance. For O_3 in particular, defining realistic mean vertical concentration profiles for the given range of T_s introduces additional uncertainty beyond the scope of this work. Continuum absorption is calculated using the latest (at the time of analysis) MT_CKD models (Mlawer et al., 2012) for water vapor (version 4.0), CO_2, N_2 (both version 2.5) and O_2 (version 1.0). At the time of writing, the only changes made since concern minor revisions of the water vapor foreign continuum in version 4.1. Consistent with MT_CKD, water vapor lines are

cut off at $25\,\mathrm{cm}^{-1}$ from the line center. Wings beyond that wavenumber and the associated "pedestal" under the line are removed, as described in detail in Clough et al. (1989).

For the sensitivity experiments, we chose a very simple approach. Apart from the reference simulation, we perform experiments in which we vary continuum absorption by spectrally uniform $\pm 10\,\%$ in the whole simulated spectral range ($10\,\mathrm{cm}^{-1}$ to $3{,}250\,\mathrm{cm}^{-1}$), as well as experiments in which self and foreign continuum are varied separately.

2.2 Forcing, feedback and climate sensitivity

For each surface temperature T_s we calculate the spectrally resolved $2\times\mathrm{CO_2}$ radiative forcing $\mathcal{F}_\nu$ by performing simulations of spectrally resolved outgoing longwave radiation $\mathcal{L}_\nu$ at two different $\mathrm{CO_2}$ concentrations: a baseline concentration of 348 ppm (note that this differs from the often-used pre-industrial value of 280 ppm) and a doubled $\mathrm{CO_2}$ concentration of 696 ppm. The forcing is then

$$\mathcal{F}_\nu(T_\mathrm{s}) = -\left[\mathcal{L}_\nu(T_\mathrm{s}, 696\,\mathrm{ppm\,CO_2}) - \mathcal{L}_\nu(T_\mathrm{s}, 348\,\mathrm{ppm\,CO_2})\right]. \tag{1}$$

Note that this forcing is defined with respect to a fixed isothermal stratosphere, in contrast to the traditional definitions of both instantaneous and effective forcing. Its numerical value is much closer (but not identical) to the literature value of effective forcing which is the relevant quantity for calculating climate sensitivity.

For each T_s we calculate the spectrally resolved longwave feedback λ_ν as the centered finite difference

$$\lambda_\nu(T_\mathrm{s}) = -\frac{\mathcal{L}_\nu(T_\mathrm{s}+1\,\mathrm{K},\ \boldsymbol{T}_{+1},\ \boldsymbol{q}_{+1}) - \mathcal{L}_\nu(T_\mathrm{s}-1\,\mathrm{K},\ \boldsymbol{T}_{-1},\ \boldsymbol{q}_{-1})}{2\,\mathrm{K}}, \tag{2}$$

where $\boldsymbol{x}_{\pm 1} = \boldsymbol{x}(T_\mathrm{s}\pm 1\,\mathrm{K})$ for the profiles of temperature $\boldsymbol{T}$ and water vapor volume mixing ratio $\boldsymbol{q}$, respectively.

The spectrally resolved surface feedback $\lambda_{\nu,\,\mathrm{sfc}}$ is defined as the change in $\mathcal{L}_\nu$ that is caused by variations in T_s alone, with $\boldsymbol{T}$ and $\boldsymbol{q}$ unchanged. Therefore, we calculate it as

$$\lambda_{\nu,\,\mathrm{sfc}}(T_\mathrm{s}) = -\frac{\mathcal{L}_\nu(T_\mathrm{s}+1\,\mathrm{K},\ \boldsymbol{T}_0,\ \boldsymbol{q}_0) - \mathcal{L}_\nu(T_\mathrm{s}-1\,\mathrm{K},\ \boldsymbol{T}_0,\ \boldsymbol{q}_0)}{2\,\mathrm{K}}, \tag{3}$$

where $\boldsymbol{x}_0 = \boldsymbol{x}(T_\mathrm{s})$ for $\boldsymbol{x} \in \{\boldsymbol{T},\, \boldsymbol{q}\}$.

The atmospheric feedback, the radiative signature of changes in $\boldsymbol{T}$ and $\boldsymbol{q}$, is calculated as

$$\lambda_{\nu,\,\mathrm{atm}}(T_\mathrm{s}) = \lambda_\nu(T_\mathrm{s}) - \lambda_{\nu,\,\mathrm{sfc}}(T_\mathrm{s}). \tag{4}$$

These spectrally resolved quantities are integrated to yield the broadband quantities as

$$x = \int_{\nu_0}^{\nu_1} x_\nu \, \mathrm{d}\nu, \tag{5}$$

where $x \in \{\mathcal{F},\, \lambda,\, \lambda_\mathrm{sfc},\, \lambda_\mathrm{atm}\}$ and $(\nu_0,\, \nu_1) = (10\,\mathrm{cm}^{-1},\, 3250\,\mathrm{cm}^{-1})$.

Finally, the longwave clear-sky climate sensitivity $\mathcal{S}$ is calculated as

$$\mathcal{S}(T_\mathrm{s}) = -\frac{\mathcal{F}(T_\mathrm{s})}{\lambda(T_\mathrm{s})}. \tag{6}$$

3 How Uncertainty in the Continuum Affects Radiative Forcing

Conceptually, the $2\times CO_2$ radiative forcing $\mathcal{F}$ depends on two factors (Jeevanjee, Seeley, et al., 2021). First, the temperature contrast between surface and stratosphere determines $\mathcal{F}$ in a dry atmosphere because surface emission is replaced with stratospheric emission at the edges of CO_2 absorption bands. Second, the presence of water vapor means that some part of the original emission originates from the troposphere rather than the surface, reducing the temperature contrast with the stratosphere and thus weakening $\mathcal{F}$. At low T_s the spectrally resolved forcing $\mathcal{F}_\nu$ is most pronounced at the edges of the major CO_2 band ($600\,\mathrm{cm}^{-1}$ to $750\,\mathrm{cm}^{-1}$). At high T_s – and thus large water vapor volume mixing ratios $\boldsymbol{q}$ – water vapor absorption masks $\mathcal{F}_\nu$ at the band edges, while the concomitant vertical expansion of the troposphere "unlocks" a substantial $\mathcal{F}_\nu$ in the band center (Kluft et al., 2021; Seeley & Jeevanjee, 2021; Jeevanjee, Seeley, et al., 2021, see also Fig. 2a). Overall, $\mathcal{F}$ increases with T_s until $T_\mathrm{s} \approx 290\,\mathrm{K}$ due to the increasing surface-stratosphere temperature contrast; at even higher T_s the weakening effect of the exponentially increasing $\boldsymbol{q}$ dominates (Kluft et al., 2021). This decrease in $\mathcal{F}$ occurs at $T_\mathrm{s} \approx$

300 K for the minor CO_2 bands in the atmospheric window around 950 cm^{-1} and 1050 cm^{-1}, and at $T_s \approx 320$ K for the major CO_2 band at 667 cm^{-1} (see Figs. 2a and 3a).

Together with water vapor line absorption, the water vapor continuum determines the atmospheric layer whose emission is replaced by stratospheric emission when CO_2 is doubled. When continuum absorption is increased, the original emission level is located at lower temperatures. Hence, the temperature contrast with the stratosphere is smaller which weakens $\mathcal{F}$, and vice versa for a decreased continuum. Consequently, the effect of the continuum on $\mathcal{F}_\nu$ is mostly limited to the edges of the CO_2 absorption bands (Fig. 2e). Due to the exponential Clausius-Clapeyron relation and the increase of continuum absorption with $\boldsymbol{q}$, the effect of the continuum on $\mathcal{F}$ increases with T_s under constant relative humidity until $T_s \approx 310$ K (Fig. 3d,g). At even higher T_s the effect of an increased continuum on the forcing contribution of the minor CO_2 bands decreases. This is because CO_2 concentration stays constant with T_s in our experiments and so the continuum absorption becomes stronger than the minor CO_2 bands at high enough T_s. In contrast, the effect of an increased continuum on the forcing contribution of the major CO_2 band continues to increase with T_s (Fig. 3d,g). The effect of the self continuum dominates throughout the spectrum; the foreign continuum only has a non-negligible effect around the major CO_2 band, which strongly decreases with T_s above 300 K (Fig. 2i,m).

At $T_s = 288$ K the effect of uncertainty in the water vapor continuum on $\mathcal{F}$ is small: An uncertainty of 10 % in continuum absorption only translates to an uncertainty in $\mathcal{F}$ of around ± 0.02 W m^{-2} (± 0.5 %). Even at $T_s = 320$ K uncertainty in $\mathcal{F}$ is only around ± 0.05 W m^{-2} (± 1 %).

4 How Uncertainty in the Continuum affects Longwave Feedback

Before we analyze the effect of uncertainty in the water vapor continuum on the longwave feedback λ, we briefly review the current understanding of its spectrally resolved counterpart λ_ν (Fig. 2b). In the atmospheric window (750 cm^{-1} to 1250 cm^{-1}), λ_ν is mostly governed by the strongly stabilizing (negative) surface feedback λ_{sfc}. However, the window continuously closes with increasing T_s which weakens λ_{sfc} and causes it to vanish at $T_s \approx 310$ K (e.g., Koll & Cronin, 2018; Kluft et al., 2021, see also Figs. 2c and 3b). Above 310 K the dependence of λ_ν in the window on water vapor volume mixing ratio $\boldsymbol{q}$ and thus on T_s is weak. This is because λ_{sfc} is replaced by a weakly destabilizing (pos-

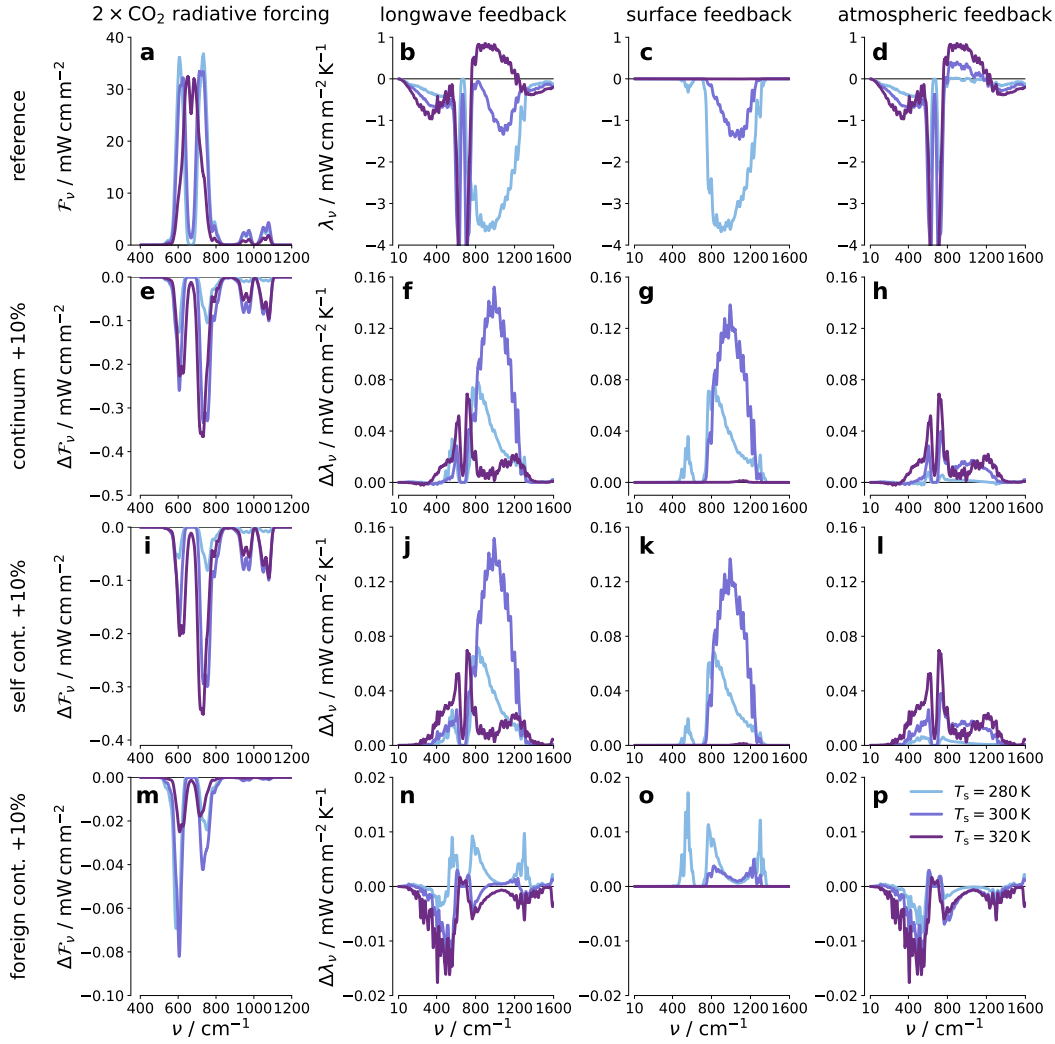

Figure 2. Effect of uncertainty in water vapor continuum on spectrally resolved 2 × CO_2 radiative forcing $\mathcal{F}_\nu$ (a, e, i, m) and longwave feedback λ_ν (b, f, j, n), which is also decomposed into surface feedback (c, g, k, o) and atmospheric feedback (d, h, l, p) for different surface temperatures T_s. Shown are the reference values (a-d), as well as the absolute changes caused by increasing the water vapor continuum by 10 % (e-h), and the isolated effects of the self continuum (i-l) and the foreign continuum (m-p).

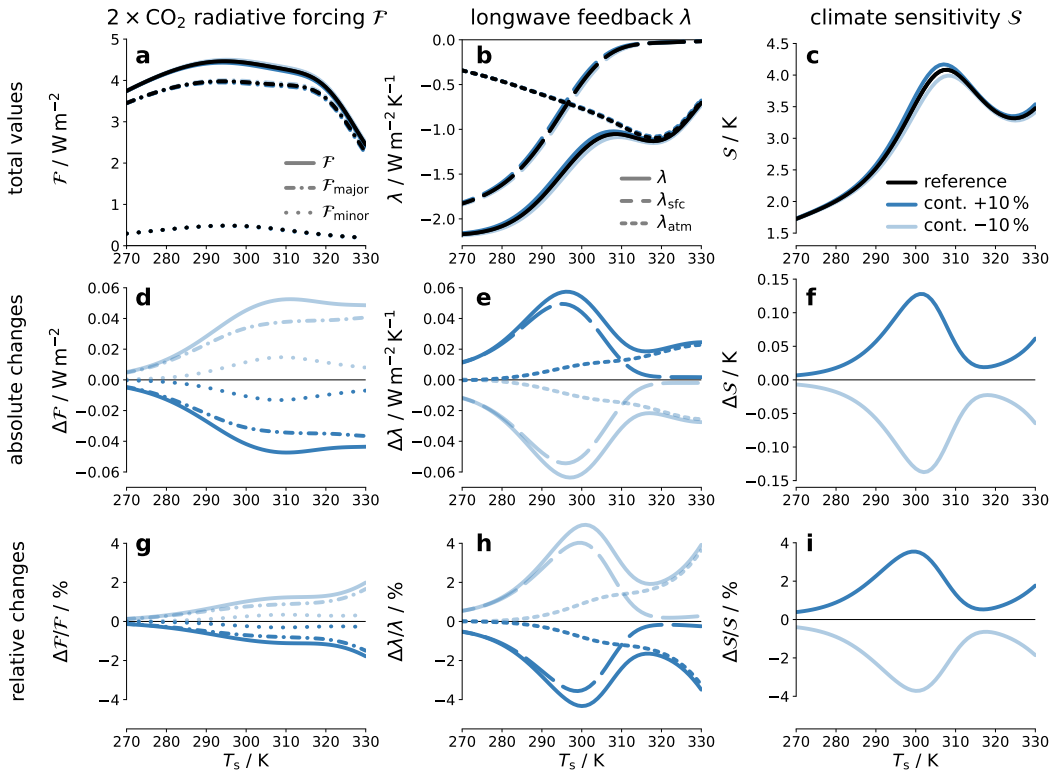

Figure 3. Effect of uncertainty in water vapor continuum on spectrally integrated 2 × CO_2 radiative forcing $\mathcal{F}$ (a, d, g), longwave feedback λ (b, e, h), and climate sensitivity $\mathcal{S}$ (c, f, i). Shown are the total values (a, b, c) of the reference simulation (black) and the simulations with varied continuum absorption (blue), as well as the absolute differences Δx (d, e, f) and relative differences $\frac{\Delta x}{x}$ (g, h, i) caused by variations in continuum absorption of +10 % (dark shading) and −10 % (light shading) for $x \in \{\mathcal{F}, \lambda, \mathcal{S}\}$. The forcing terms are split into the contribution by the major CO_2 band $\mathcal{F}_{\text{major}}$ ($\nu < 900\,\text{cm}^{-1}$, dash-dotted) and minor CO_2 bands $\mathcal{F}_{\text{minor}}$ ($\nu > 900\,\text{cm}^{-1}$, loosely dotted); the feedback terms are split into surface feedback λ_{sfc} (dashed) and atmospheric feedback λ_{atm} (dotted).

itive) atmospheric feedback λ_{atm} caused by the water vapor continuum which is described in more detail below (Koll et al., 2023, see also Figs. 2d and 3b).

Outside the window region, λ_ν is almost entirely determined by λ_{atm}. In the major CO_2 band ($600\,\mathrm{cm}^{-1}$ to $750\,\mathrm{cm}^{-1}$), λ_{atm} is close to zero at present-day T_s as the emission level there is located in the stratosphere but becomes strongly stabilizing at high T_s due to the vertical expansion of the troposphere. This stabilizing λ_{atm} is strongest at the band edges but also reaches the band center at $T_\mathrm{s} > 300\,\mathrm{K}$. At $T_\mathrm{s} > 320\,\mathrm{K}$ the stabilizing λ_{atm} is weakened due to masking by water vapor absorption (Kluft et al., 2021; Seeley & Jeevanjee, 2021, see also Figs. 2d and 3b).

Finally, λ_{atm} is weakly stabilizing in the water vapor bands in the far-infrared (FIR, $200\,\mathrm{cm}^{-1}$ to $600\,\mathrm{cm}^{-1}$) and mid-infrared (MIR, $1250\,\mathrm{cm}^{-1}$ to $2000\,\mathrm{cm}^{-1}$), which are dominated by water vapor line absorption. Here, the first-order approximation of a roughly constant emission temperature which would imply a neutral λ_{atm} (Simpson, 1928b, 1928a; Ingram, 2010; Jeevanjee, Koll, & Lutsko, 2021) does not hold entirely due to effects like pressure broadening which induce a weakly stabilizing λ_{atm} (Feng et al., 2023; Koll et al., 2023, see also Fig. 2d).

Water vapor continuum absorption affects λ by altering both λ_{sfc} and λ_{atm} (Koll et al., 2023). In the following, we therefore discuss the partial feedback induced by an increase in the continuum of 10 %. A destabilizing partial feedback means that the total feedback becomes less stabilizing, and vice versa. The continuum dampens the stabilizing λ_{sfc} in the atmospheric window by damping surface emission. Hence, a stronger continuum dampens λ_{sfc} more and thus induces a destabilizing partial feedback at $T_\mathrm{s} < 310\,\mathrm{K}$, when the window is still open, and vice versa for a weaker continuum (Fig. 2g). This destabilizing partial feedback can be seen for both continuum components, but the effect of the self continuum (Fig. 2k) is much stronger than that of the foreign continuum (Fig. 2o).

The continuum affects λ_{atm} because its emission temperature is sensitive to the temperature lapse rate. The decreasing lapse rate with increasing T_s additionally increases $\boldsymbol{q}$. This in turn causes the continuum to emit at lower temperatures, giving rise to a destabilizing lapse-rate feedback (Koll et al., 2023). The effect of an increased continuum on λ_{atm} is weaker than that on λ_{sfc} below $T_\mathrm{s} \approx 310\,\mathrm{K}$ but becomes the dominant effect at higher T_s (Fig. 3e). Below $T_\mathrm{s} \approx 300\,\mathrm{K}$ the effect on λ_{atm} is mostly limited to the atmo-

spheric window but it also reaches the absorption bands of water vapor and CO_2 at higher T_s. This destabilizing effect of an increased continuum on λ_{atm} continuously increases with T_s in both H_2O and CO_2 absorption bands, while in the window it peaks at around 300 K and slowly decreases at higher T_s (Fig. 2h). Furthermore, in contrast to the self continuum (Fig. 2l), the foreign continuum has a weakly stabilizing effect on λ_{atm}, particularly in the FIR water vapor band (Fig. 2p).

The stabilizing effect of a foreign continuum increase might seem surprising at first. To understand it, and also the other described changes, it is useful to think of them as resulting from shifts in the absorption species that control the main spectral regions as T_s increases. To demonstrate this, we calculate the spectrally resolved opacity $\tau_\nu(s, p)$ of each absorbing species s from the top of the atmosphere (TOA) to each pressure level p based on the line-by-line simulations. We consider both the total H_2O continuum and the self and foreign continuum separately. The emission pressure $p_{em,\nu}(s)$ of each species is then defined as the largest p where $\tau_\nu(s, p) \leq 1$ (as seen from TOA). From this, we define the "emitting" species at each wavenumber ν as the species with the smallest $p_{em,\nu}(s)$. If no species has $\tau_\nu(s) > 0.5$ at the surface, no "emitting" species is chosen for that wavenumber; if multiple species have the same $p_{em,\nu}(s)$, all of them are defined as "emitting" species. We separately consider three main spectral regions of interest: the FIR water vapor band, the major CO_2 band, and the atmospheric window. The emission fraction $f_{em}(s, T_s)$ is the fraction of all simulated wavenumbers within each of those bands at which each species s is the "emitting" species, estimating which species most strongly impacts atmospheric emission and thus λ at a given T_s.

Using both the opacity of the entire atmospheric column τ and the emission fraction f_{em} of the analyzed species, we analyze the effect of uncertainty in the continuum on outgoing longwave radiation $\mathcal{L}$ and thus longwave feedback λ. This setup allows us to explain (1) differences between self and foreign continuum, (2) differences between spectral bands, and (3) dependence on surface temperature T_s (Fig. 4). The explanation relies on the dependences of the opacity of the different absorbing species on $\boldsymbol{q}$ and thus on T_s under constant relative humidity (Fig. 4 first column) which can be expressed as

$$\frac{d\log(\tau_{self})}{dT_s} > \frac{d\log(\tau_{continuum})}{dT_s} > \frac{d\log(\tau_{H_2O\ lines})}{dT_s} > \frac{d\log(\tau_{foreign})}{dT_s} > \frac{d\log(\tau_{CO_2})}{dT_s}. \quad (7)$$

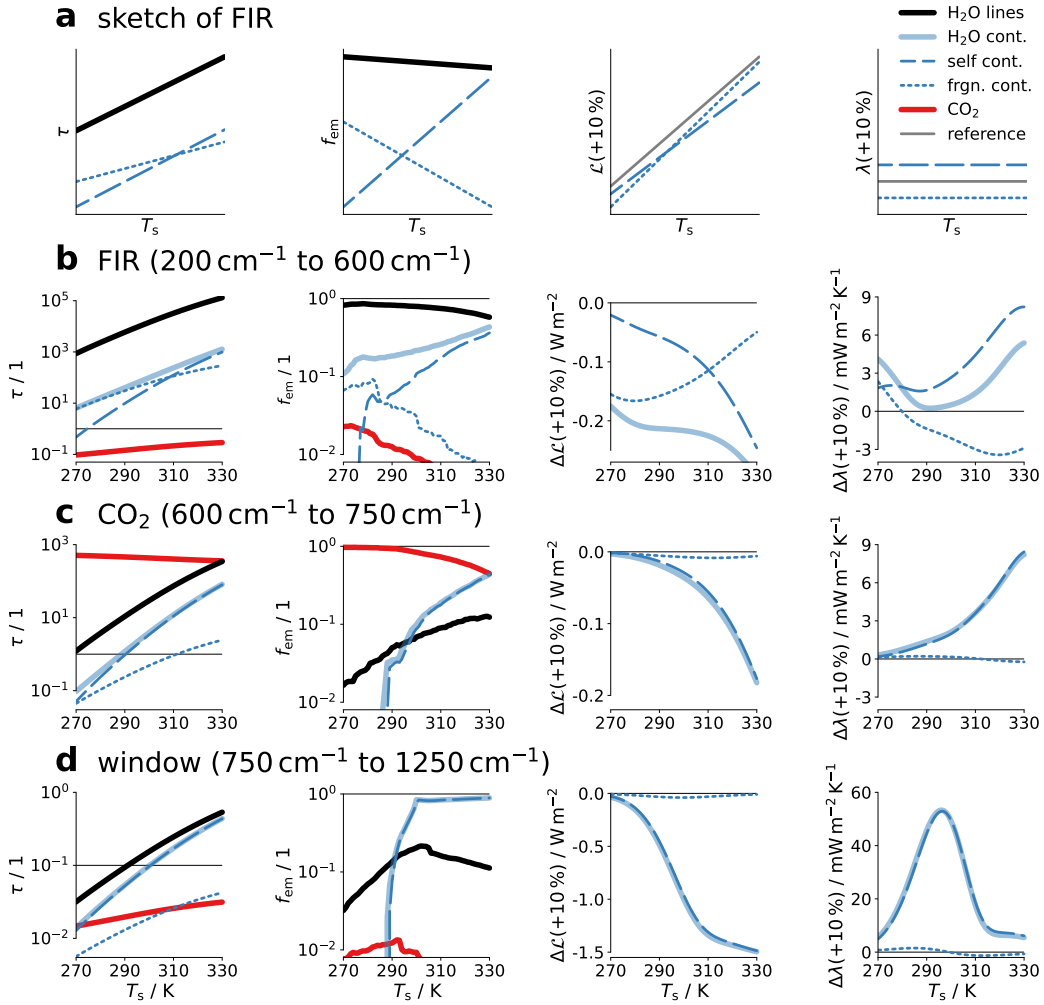

Figure 4. Band-averaged opacity τ (first column), band emission fraction f_{em} (second column), band-integrated outgoing longwave radiation $\mathcal{L}$ (third column), and band-integrated longwave feedback λ (fourth column). An idealized sketch of the mechanism in the far-infrared (FIR) water vapor absorption band is shown in the first row. Below, the actual values are shown for the FIR band, the major CO_2 band, and the atmospheric window. Note that the results shown in the third and fourth columns represent the changes in $\mathcal{L}$ and λ caused by increasing the continuum (self, foreign, and combined) by 10 %, except for the first row where the absolute values of $\mathcal{L}$ and λ are sketched.

Regarding the differences between the partial feedbacks of self and foreign continuum, the implications of equation (7) are sketched for the FIR water vapor band (Fig. 4a). The strong T_s dependence of τ(self) means that the self continuum "gains ground" compared to the other species and thus f_{em}(self) strongly increases with T_s. In contrast, the weak T_s dependence of τ(foreign) means that the foreign continuum "loses ground" compared to the other species and thus f_{em}(foreign) decreases with T_s. Accordingly, a stronger self continuum mostly reduces $\mathcal{L}$ at high T_s, while a stronger foreign continuum mostly reduces $\mathcal{L}$ at low T_s. Hence, the slope of $\mathcal{L}$ against T_s becomes flatter (less stabilizing) as the self continuum is increased but steeper (more stabilizing) as the foreign continuum is increased. In other words, the self continuum induces a destabilizing partial feedback while the foreign continuum induces a stabilizing partial feedback. At present-day T_s these partial feedbacks roughly cancel, at higher T_s the destabilizing self continuum partial feedback dominates (Fig. 4b).

Outside the water vapor bands, the partial feedback induced by the foreign continuum is negligible. Nevertheless, this framework can also help us understand why the continuum partial feedback varies between different spectral bands and with T_s. In contrast to the exponential Clausius-Clapeyron relation imposed on water vapor, CO_2 concentration stays constant with T_s in our experiments. Hence, f_{em}(continuum) in the CO_2 band strongly increases with T_s at the cost of CO_2 absorption. Therefore, the destabilizing lapse-rate feedback induced by the continuum continuously masks more of the stabilizing Planckian response induced by CO_2 at the edges of the $667\,cm^{-1}$ CO_2 band, above $T_s \approx 320\,K$ this effect even reaches the band center (Figs. 2h and 4c).

In the window, f_{em}(continuum) also increases with T_s along with the continuum partial feedback. At $T_s \approx 300\,K$, however, f_{em}(continuum) $\sim \mathcal{O}(1)$ which means that the continuum controls most of the emission in the window. Further increasing T_s thus leads to a much weaker increase in f_{em}(continuum) than below 300 K and thus the continuum's destabilizing effect weakens (Fig. 4d).

Overall, uncertainty in λ caused by the water vapor continuum strongly varies with T_s. At $T_s = 288\,K$ a 10 % stronger continuum causes λ to become $0.04\,W\,m^{-2}\,K^{-1}$ (2.5 %) less negative. This uncertainty continuously increases with T_s and reaches a maximum of $0.06\,W\,m^{-2}\,K^{-1}$ (4 %) around 300 K. Most of this uncertainty stems from the atmospheric window, where a stronger continuum weakens λ_{window} by about $0.04\,W\,m^{-2}\,K^{-1}$

on average between 290 K and 310 K. Because λ_{window} weakens by about $0.05\,\text{W}\,\text{m}^{-2}\,\text{K}^{-2}$ as T_s increases, the continuum uncertainty induces an uncertainty in the T_s at which the atmospheric window closes of about ± 0.8 K. Phrased differently, because the opacity τ of continuum absorption continuously increases with T_s (Figs. 1a and 4 first column), variations in the continuum strength can be thought of as shifting τ in T_s space – and thus also the T_s at which the window closes.

5 Implications for Climate Sensitivity and General Discussion

The T_s dependence of climate sensitivity $\mathcal{S}$ (Fig. 3c) can be understood from the T_s dependence of radiative forcing $\mathcal{F}$ and longwave feedback λ (see Secs. 3 and 4, also e.g., Kluft et al., 2021). The effects of uncertainty in the continuum on $\mathcal{F}$ and λ have opposing effects on $\mathcal{S}$. The weaker $\mathcal{F}$ favors a lower $\mathcal{S}$, while the weaker λ favors a higher $\mathcal{S}$. The effect of λ clearly dominates, causing $\mathcal{S}$ to increase for a stronger continuum and vice versa. At $T_\text{s} = 288$ K increasing the continuum by 10 % increases $\mathcal{S}$ by 0.05 K (2 %); at $T_\text{s} = 300$ K this sensitivity more than doubles to 0.13 K (4 %).

Although the effect of continuum variations on $\mathcal{F}$, λ, and $\mathcal{S}$ is largely symmetric regarding the sign of the change there are some deviations from this symmetry: For a decrease in the continuum of 10 %, $\mathcal{F}$ changes on average about 7 % more, λ about 10 % more, and $\mathcal{S}$ about 5 % more than for an increase in the continuum of 10 %. Nonlinearity is also present when it comes to applying our results to different assumed uncertainties. A doubled uncertainty in the water vapor continuum of ± 20 % does not quite double the resulting uncertainty in $\mathcal{F}$, λ, and $\mathcal{S}$, although the deviations are less than 10 % (not shown).

6 Conclusions

We assess the effect of uncertainty in water vapor continuum absorption on 2 × CO_2 radiative forcing $\mathcal{F}$, longwave feedback λ, and climate sensitivity $\mathcal{S}$. To this end, we perform radiative-convective equilibrium simulations at different surface temperatures T_s, assuming moist adiabatic temperature profiles (isothermal above 175 K) and 80 % relative humidity. Based on these profiles, we perform line-by-line radiative transfer simulations of the spectral outgoing longwave radiation $\mathcal{L}_\nu$, assuming a spectrally uniform uncertainty of ± 10 % in water vapor continuum absorption.

A 10 % stronger continuum destabilizes λ by dampening the surface feedback in the atmospheric window at $T_s < 310\,\mathrm{K}$ and by inducing an atmospheric lapse-rate feedback particularly at $T_s > 300\,\mathrm{K}$, consistent with Koll et al. (2023). This atmospheric feedback is also present in the absorption bands of water vapor and CO_2 due to the continuum's stronger T_s dependence compared to line absorption by water vapor and CO_2. Overall, uncertainty in the continuum has a much stronger effect on λ than on $\mathcal{F}$. Both $\mathcal{F}$ and λ are weaker for a stronger continuum which induces opposite effects on $\mathcal{S}$. Under present-day conditions, $\mathcal{S}$ increases by about $0.05\,\mathrm{K}$ (2 %) for a 10 % stronger continuum. When the atmospheric window closes at $T_s \approx 300\,\mathrm{K}$ this uncertainty reaches $0.13\,\mathrm{K}$ (4 %).

Both self and foreign continuum have a weakening effect on $\mathcal{F}$ when increased. In contrast, while an increased self continuum has a destabilizing effect on λ, an increased foreign continuum has a weakly stabilizing effect due to its relatively weak T_s dependence, as described above. This implies that λ – and thus $\mathcal{S}$ – is sensitive not only to uncertainty in the absolute magnitude of the continuum but also to uncertainty in the partitioning between self- and foreign continua.

Overall, uncertainty caused by continuum absorption is small compared to the main uncertainties affecting $\mathcal{S}$, such as the effects of clouds and aerosols (Sherwood et al., 2020). However, the longwave clear-sky $\mathcal{S}$ can be estimated with much higher accuracy, with a canonical value of around 2 K and a small uncertainty of generally less than 10 % (Manabe & Wetherald, 1967; Kluft et al., 2019; Stevens & Kluft, 2023; Jeevanjee, 2023). Therefore, when it comes to constraining this clear-sky longwave $\mathcal{S}$, uncertainty in water vapor continuum absorption appears to be of comparable magnitude to other remaining uncertainties. In particular, this uncertainty is non-negligible for analyzing the temperature dependence of the clear-sky longwave $\mathcal{S}$.

7 Open Research

Our analysis is based on the konrad model version 1.0.1 (available at 10.5281/zenodo.6046423, Kluft et al., 2022), with some modifications to the model to support the scaling of absorption species (available at 10.5281/zenodo.8060484, Roemer et al., 2023a). For the radiative transfer simulations, we use the ARTS model version 2.5.10 (available at 10.5281/zenodo.8004364, Buehler et al., 2023). The model output produced in this study can be found at 10.5281/zenodo.8046651 (Roemer et al., 2023c), the code needed to run the models and produce the figures of this study can be found at 10.5281/zenodo.8046932 (Roemer et al., 2023b).

Acknowledgments

This work was financially supported by the US National Science Foundation (award AGS-1916908) and by NOAA (award NA20OAR4310375). This study contributes to the Cluster of Excellence 'CLICCS—Climate, Climatic Change, and Society', and to the Center for Earth System Research and Sustainability (CEN) of Universität Hamburg. We want to thank Richard Larsson for developing the ARTS absorption routines, including their representation of the MT_CKD continuum. Our thanks also go to Manfred Brath, Oliver Lemke, and the ARTS radiative transfer community for their help with using ARTS.

References

Baranov, Y. I., Lafferty, W. J., Ma, Q., & Tipping, R. H. (2008, August). Water-vapor continuum absorption in the 800–1250cm-1 spectral region at temperatures from 311 to 363K. *Journal of Quantitative Spectroscopy and Radiative Transfer*, *109*(12), 2291–2302. Retrieved 2022-10-05, from `https://www.sciencedirect.com/science/article/pii/S0022407308000642` doi: 10.1016/j.jqsrt.2008.03.004

Buehler, S. A., Eriksson, P., Lemke, O., Larsson, R., Pfreundschuh, S., & Brath, M. (2023, February). *ARTS - The Atmospheric Radiative Transfer Simulator Prerelease 2.5.10.* Zenodo. Retrieved 2023-06-14, from `https://zenodo.org/record/8004364` (Language: eng) doi: 10.5281/zenodo.8004364

Buehler, S. A., Mendrok, J., Eriksson, P., Perrin, A., Larsson, R., & Lemke, O. (2018, April). ARTS, the Atmospheric Radiative Transfer Simulator – version 2.2, the planetary toolbox edition. *Geoscientific Model*

Development, *11*(4), 1537–1556. Retrieved 2023-05-11, from https://gmd.copernicus.org/articles/11/1537/2018/ (Publisher: Copernicus GmbH) doi: 10.5194/gmd-11-1537-2018

Burch, D. E. (1982). *Continuum Absorption by H2O.* (Tech. Rep.). Retrieved 2023-05-26, from https://apps.dtic.mil/sti/citations/ADA112264 (Section: Technical Reports)

Burch, D. E., & Alt, R. L. (1984). *Continuum Absorption by H2O in the 700-1200 cm(-1) and 2400-2800 cm(-1) Windows,* (Tech. Rep.). Retrieved 2022-10-05, from https://apps.dtic.mil/sti/citations/ADA147391 (Section: Technical Reports)

Clough, S. A., Kneizys, F. X., & Davies, R. W. (1989, October). Line shape and the water vapor continuum. *Atmospheric Research*, *23*(3), 229–241. Retrieved 2022-10-05, from https://www.sciencedirect.com/science/article/pii/0169809589900203 doi: 10.1016/0169-8095(89)90020-3

Cormier, J. G., Hodges, J. T., & Drummond, J. R. (2005, March). Infrared water vapor continuum absorption at atmospheric temperatures. *The Journal of Chemical Physics*, *122*(11), 114309. Retrieved 2022-10-05, from https://aip.scitation.org/doi/10.1063/1.1862623 (Publisher: American Institute of Physics) doi: 10.1063/1.1862623

Dacie, S., Kluft, L., Schmidt, H., Stevens, B., Buehler, S. A., Nowack, P. J., ... Birner, T. (2019, October). A 1D RCE Study of Factors Affecting the Tropical Tropopause Layer and Surface Climate. *Journal of Climate*, *32*(20), 6769–6782. Retrieved 2023-05-16, from https://journals.ametsoc.org/view/journals/clim/32/20/jcli-d-18-0778.1.xml (Publisher: American Meteorological Society Section: Journal of Climate) doi: 10.1175/JCLI-D-18-0778.1

Eng, R. S., & Mantz, A. W. (1980). Tunable diode laser measurements of water vapor continuum and water vapor absorption line shape in the 10 μm atmospheric transmission window region. In *Atmospheric water vapor* (pp. 101–111). Elsevier.

Eriksson, P., Buehler, S. A., Davis, C. P., Emde, C., & Lemke, O. (2011, July). ARTS, the atmospheric radiative transfer simulator, version 2. *Journal of Quantitative Spectroscopy and Radiative Transfer*, *112*(10), 1551–1558. Retrieved 2023-05-11, from https://www.sciencedirect.com/science/

article/pii/S0022407311001105 doi: 10.1016/j.jqsrt.2011.03.001

Feng, J., Paynter, D., & Menzel, R. (2023). How a Stable Greenhouse Effect on Earth Is Maintained Under Global Warming. *Journal of Geophysical Research: Atmospheres*, *128*(9), e2022JD038124. Retrieved 2023-06-16, from https://onlinelibrary.wiley.com/doi/abs/10.1029/2022JD038124 (_eprint: https://onlinelibrary.wiley.com/doi/pdf/10.1029/2022JD038124) doi: 10.1029/2022JD038124

Hinderling, J., Sigrist, M. W., & Kneubühl, F. K. (1987, March). Laser-photoacoustic spectroscopy of water-vapor continuum and line absorption in the 8 to 14 μm atmospheric window. *Infrared Physics*, *27*(2), 63–120. Retrieved 2023-05-31, from https://www.sciencedirect.com/science/article/pii/0020089187900133 doi: 10.1016/0020-0891(87)90013-3

Ingram, W. (2010). A very simple model for the water vapour feedback on climate change. *Quarterly Journal of the Royal Meteorological Society*, *136*(646), 30–40. Retrieved 2023-04-14, from https://onlinelibrary.wiley.com/doi/abs/10.1002/qj.546 (_eprint: https://onlinelibrary.wiley.com/doi/pdf/10.1002/qj.546) doi: 10.1002/qj.546

Jeevanjee, N. (2023, May). *Climate sensitivity from radiative-convective equilibrium: a blackboard approach* (preprint). Preprints. Retrieved 2023-06-16, from https://essopenarchive.org/users/529276/articles/626552-climate-sensitivity-from-radiative-convective-equilibrium-a-blackboard-approach?commit=5c537c42d7a322686aa3079790c21d2cc02c3f4b doi: 10.22541/au.167752745.56200468/v2

Jeevanjee, N., Koll, D. D. B., & Lutsko, N. (2021). "Simpson's Law" and the Spectral Cancellation of Climate Feedbacks. *Geophysical Research Letters*, *48*(14), e2021GL093699. Retrieved 2022-09-26, from https://onlinelibrary.wiley.com/doi/abs/10.1029/2021GL093699 (_eprint: https://onlinelibrary.wiley.com/doi/pdf/10.1029/2021GL093699) doi: 10.1029/2021GL093699

Jeevanjee, N., Seeley, J. T., Paynter, D., & Fueglistaler, S. (2021, December). An Analytical Model for Spatially Varying Clear-Sky CO2 Forcing. *Journal of Climate*, *34*(23), 9463–9480. Retrieved 2023-05-11, from https://journals.ametsoc.org/view/journals/clim/34/23/JCLI-D-19-0756.1.xml

(Publisher: American Meteorological Society Section: Journal of Climate) doi: 10.1175/JCLI-D-19-0756.1

Kluft, L., Dacie, S., & Bourdin, S. (2022, February). *atmtools/konrad: Fix ARTS and cloud interfaces.* Zenodo. Retrieved 2023-05-11, from `https://zenodo.org/record/6046423` doi: 10.5281/zenodo.6046423

Kluft, L., Dacie, S., Brath, M., Buehler, S. A., & Stevens, B. (2021). Temperature-Dependence of the Clear-Sky Feedback in Radiative-Convective Equilibrium. *Geophysical Research Letters*, *48*(22), e2021GL094649. Retrieved 2023-03-16, from `https://onlinelibrary.wiley.com/doi/abs/10.1029/2021GL094649` (_eprint: https://onlinelibrary.wiley.com/doi/pdf/10.1029/2021GL094649) doi: 10.1029/2021GL094649

Kluft, L., Dacie, S., Buehler, S. A., Schmidt, H., & Stevens, B. (2019, December). Re-Examining the First Climate Models: Climate Sensitivity of a Modern Radiative–Convective Equilibrium Model. *Journal of Climate*, *32*(23), 8111–8125. Retrieved 2023-05-11, from `https://journals.ametsoc.org/view/journals/clim/32/23/jcli-d-18-0774.1.xml` (Publisher: American Meteorological Society Section: Journal of Climate) doi: 10.1175/JCLI-D-18-0774.1

Koll, D. D. B., & Cronin, T. W. (2018, October). Earth's outgoing longwave radiation linear due to H2O greenhouse effect. *Proceedings of the National Academy of Sciences*, *115*(41), 10293–10298. Retrieved 2023-05-11, from `https://www.pnas.org/doi/10.1073/pnas.1809868115` (Publisher: Proceedings of the National Academy of Sciences) doi: 10.1073/pnas.1809868115

Koll, D. D. B., Jeevanjee, N., & Lutsko, N. J. (2023, April). An Analytic Model for the Clear-Sky Longwave Feedback. *Journal of the Atmospheric Sciences*, *-1*(aop). Retrieved 2023-05-31, from `https://journals.ametsoc.org/view/journals/atsc/aop/JAS-D-22-0178.1/JAS-D-22-0178.1.xml` (Publisher: American Meteorological Society Section: Journal of the Atmospheric Sciences) doi: 10.1175/JAS-D-22-0178.1

Loper, G. L., O'Neill, M. A., & Gelbwachs, J. A. (1983, December). Water-vapor continuum CO_2 laser absorption spectra between 27°C and -10°C. *Applied Optics*, *22*(23), 3701–3710. Retrieved 2023-05-31, from `https://opg.optica.org/ao/abstract.cfm?uri=ao-22-23-3701` (Publisher: Optica Publishing Group) doi: 10.1364/AO.22.003701

Manabe, S., & Wetherald, R. T. (1967, May). Thermal Equilibrium of the Atmosphere with a Given Distribution of Relative Humidity. *Journal of the Atmospheric Sciences*, *24*(3), 241–259. Retrieved 2023-04-17, from http://journals.ametsoc.org/doi/10.1175/1520-0469(1967)024<0241:TEOTAW>2.0.CO;2 doi: 10.1175/1520-0469(1967)024⟨0241:TEOTAW⟩2.0.CO;2

Meraner, K., Mauritsen, T., & Voigt, A. (2013). Robust increase in equilibrium climate sensitivity under global warming. *Geophysical Research Letters*, *40*(22), 5944–5948. Retrieved 2023-05-12, from https://onlinelibrary.wiley.com/doi/abs/10.1002/2013GL058118 (_eprint: https://onlinelibrary.wiley.com/doi/pdf/10.1002/2013GL058118) doi: 10.1002/2013GL058118

Mlawer, E. J., Payne, V. H., Moncet, J.-L., Delamere, J. S., Alvarado, M. J., & Tobin, D. C. (2012, June). Development and recent evaluation of the MT_ckd model of continuum absorption. *Philosophical Transactions of the Royal Society A: Mathematical, Physical and Engineering Sciences*, *370*(1968), 2520–2556. Retrieved 2022-10-06, from https://royalsocietypublishing.org/doi/10.1098/rsta.2011.0295 doi: 10.1098/rsta.2011.0295

Nordstrom, R. J., Thomas, M. E., Peterson, J. C., Damon, E. K., & Long, R. K. (1978, September). Effects of oxygen addition on pressure-broadened water-vapor absorption in the 10-microm region. *Applied Optics*, *17*(17), 2724–2729. doi: 10.1364/AO.17.002724

Odintsova, T. A., Koroleva, A. O., Simonova, A. A., Campargue, A., & Tretyakov, M. Y. (2022, April). The atmospheric continuum in the "terahertz gap" region (15–700 cm-1): Review of experiments at SOLEIL synchrotron and modeling. *Journal of Molecular Spectroscopy*, *386*, 111603. Retrieved 2023-05-25, from https://www.sciencedirect.com/science/article/pii/S0022285222000285 doi: 10.1016/j.jms.2022.111603

Paynter, D. J., Ptashnik, I. V., Shine, K. P., Smith, K. M., McPheat, R., & Williams, R. G. (2009). Laboratory measurements of the water vapor continuum in the 1200–8000 cm-1 region between 293 K and 351 K. *Journal of Geophysical Research: Atmospheres*, *114*(D21). Retrieved 2023-05-15, from https://onlinelibrary.wiley.com/doi/abs/10.1029/2008JD011355 (_eprint: https://onlinelibrary.wiley.com/doi/pdf/10.1029/2008JD011355) doi:

10.1029/2008JD011355

Paynter, D. J., & Ramaswamy, V. (2011). An assessment of recent water vapor continuum measurements upon longwave and shortwave radiative transfer. *Journal of Geophysical Research: Atmospheres*, *116*(D20). Retrieved 2022-10-06, from https://onlinelibrary.wiley.com/doi/abs/10.1029/2010JD015505 (_eprint: https://onlinelibrary.wiley.com/doi/pdf/10.1029/2010JD015505) doi: 10.1029/2010JD015505

Paynter, D. J., & Ramaswamy, V. (2012, August). Variations in water vapor continuum radiative transfer with atmospheric conditions: WATER VAPOR CONTINUUM ENERGY BUDGET. *Journal of Geophysical Research: Atmospheres*, *117*(D16), n/a–n/a. Retrieved 2022-10-06, from http://doi.wiley.com/10.1029/2012JD017504 doi: 10.1029/2012JD017504

Peterson, J. C., Thomas, M. E., Nordstrom, R. J., Damon, E. K., & Long, R. K. (1979, March). Water vapor-nitrogen absorption at CO(2) laser frequencies. *Applied Optics*, *18*(6), 834–841. doi: 10.1364/AO.18.000834

Ptashnik, I., Shine, K., & Vigasin, A. (2011, May). Water vapour self-continuum and water dimers: 1. Analysis of recent work. *Journal of Quantitative Spectroscopy and Radiative Transfer*, *112*(8), 1286–1303. Retrieved 2023-02-16, from https://linkinghub.elsevier.com/retrieve/pii/S0022407311000379 doi: 10.1016/j.jqsrt.2011.01.012

Roemer, F. E., Buehler, S. A., Kluft, L., & Pincus, R. (2023a, June). *Git Patches to modify konrad to support scaling of absorption species in line-by-line calculations.* Zenodo. Retrieved 2023-06-20, from https://zenodo.org/record/8060484 (Language: eng) doi: 10.5281/zenodo.8060484

Roemer, F. E., Buehler, S. A., Kluft, L., & Pincus, R. (2023b, June). *Supplementary code for "Effect of Uncertainty in Water Vapor Continuum Absorption on Radiative Forcing, Longwave Feedback and Climate Sensitivity".* Zenodo. Retrieved 2023-06-20, from https://zenodo.org/record/8046932 (Language: eng) doi: 10.5281/zenodo.8046932

Roemer, F. E., Buehler, S. A., Kluft, L., & Pincus, R. (2023c, June). *Supplementary data for "Effect of Uncertainty in Water Vapor Continuum Absorption on Radiative Forcing, Longwave Feedback and Climate Sensitivity".* Zenodo. Retrieved 2023-06-20, from https://zenodo.org/record/8046651 doi:

10.5281/zenodo.8046651

Romps, D. M. (2020, March). Climate Sensitivity and the Direct Effect of Carbon Dioxide in a Limited-Area Cloud-Resolving Model. *Journal of Climate*, *33*(9), 3413–3429. Retrieved 2023-05-12, from https://journals.ametsoc.org/view/journals/clim/33/9/jcli-d-19-0682.1.xml (Publisher: American Meteorological Society Section: Journal of Climate) doi: 10.1175/JCLI-D-19-0682.1

Seeley, J. T., & Jeevanjee, N. (2021). H2O Windows and CO2 Radiator Fins: A Clear-Sky Explanation for the Peak in Equilibrium Climate Sensitivity. *Geophysical Research Letters*, *48*(4), e2020GL089609. Retrieved 2023-04-13, from https://onlinelibrary.wiley.com/doi/abs/10.1029/2020GL089609 (_eprint: https://onlinelibrary.wiley.com/doi/pdf/10.1029/2020GL089609) doi: 10.1029/2020GL089609

Sherwood, S. C., Webb, M. J., Annan, J. D., Armour, K. C., Forster, P. M., Hargreaves, J. C., ... Zelinka, M. D. (2020). An Assessment of Earth's Climate Sensitivity Using Multiple Lines of Evidence. *Reviews of Geophysics*, *58*(4), e2019RG000678. Retrieved 2023-05-11, from https://onlinelibrary.wiley.com/doi/abs/10.1029/2019RG000678 (_eprint: https://onlinelibrary.wiley.com/doi/pdf/10.1029/2019RG000678) doi: 10.1029/2019RG000678

Shine, K. P., Campargue, A., Mondelain, D., McPheat, R. A., Ptashnik, I. V., & Weidmann, D. (2016, September). The water vapour continuum in near-infrared windows – Current understanding and prospects for its inclusion in spectroscopic databases. *Journal of Molecular Spectroscopy*, *327*, 193–208. Retrieved 2022-10-04, from https://www.sciencedirect.com/science/article/pii/S0022285216300637 doi: 10.1016/j.jms.2016.04.011

Shine, K. P., Ptashnik, I. V., & Rädel, G. (2012, July). The Water Vapour Continuum: Brief History and Recent Developments. *Surveys in Geophysics*, *33*(3), 535–555. Retrieved 2022-10-04, from https://doi.org/10.1007/s10712-011-9170-y doi: 10.1007/s10712-011-9170-y

Simpson, G. (1928a). Further studies in terrestrial radiation. *Mem. R. Meteorol. Soc*, *3*, 1–26.

Simpson, G. (1928b). Some studies in terrestrial radiation. *Mem. R. Meteorol. Soc*,

2, 69–95.

Stevens, B., & Kluft, L. (2023, January). A Colorful look at Climate Sensitivity. *EGUsphere*, 1–24. Retrieved 2023-03-16, from https://egusphere.copernicus.org/preprints/2023/egusphere-2022-1460/ (Publisher: Copernicus GmbH) doi: 10.5194/egusphere-2022-1460

Taylor, J. P., Newman, S. M., Hewison, T. J., & McGrath, A. (2003, October). Water vapour line and continuum absorption in the thermal infrared—reconciling models and observations. *Quarterly Journal of the Royal Meteorological Society*, *129*(594), 2949–2969. Retrieved 2023-02-14, from http://doi.wiley.com/10.1256/qj.03.08 doi: 10.1256/qj.03.08

Tipping, R. H., & Ma, Q. (1995, March). Theory of the water vapor continuum and validations. *Atmospheric Research*, *36*(1), 69–94. Retrieved 2023-05-15, from https://www.sciencedirect.com/science/article/pii/016980959400028C doi: 10.1016/0169-8095(94)00028-C

Figure 1.

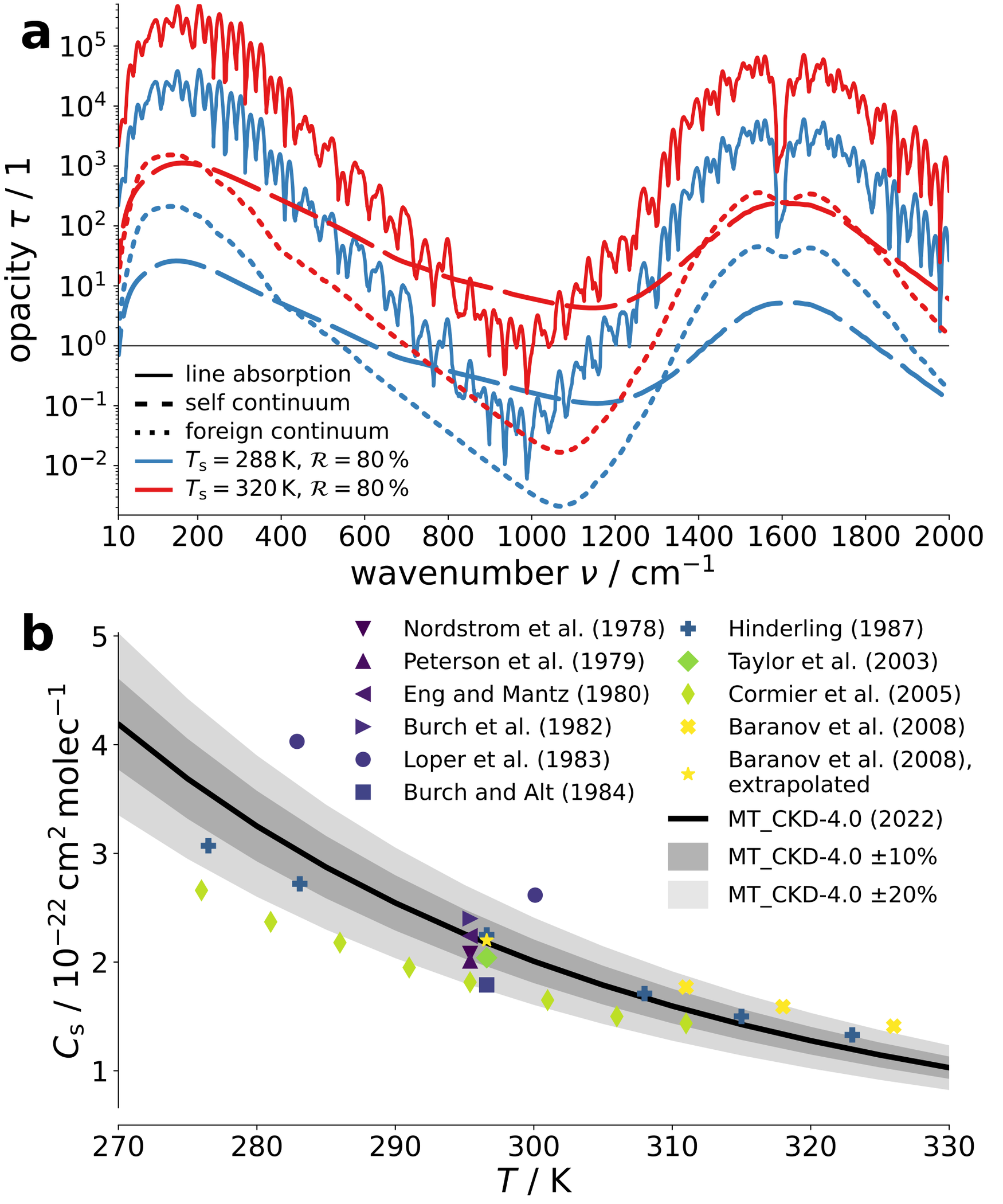
a
opacity τ / 1
10^5
10^4
10^3
10^2
10^1
10^0
10^{-1}
10^{-2}
line absorption
self continuum
foreign continuum
$T_s = 288\,\mathrm{K}$, $\mathcal{R} = 80\,\%$
$T_s = 320\,\mathrm{K}$, $\mathcal{R} = 80\,\%$
10 200 400 600 800 1000 1200 1400 1600 1800 2000
wavenumber ν / cm^{-1}
b
C_s / $10^{-22}\,\mathrm{cm}^2\,\mathrm{molec}^{-1}$
1 2 3 4 5
Nordstrom et al. (1978)
Peterson et al. (1979)
Eng and Mantz (1980)
Burch et al. (1982)
Loper et al. (1983)
Burch and Alt (1984)
Hinderling (1987)
Taylor et al. (2003)
Cormier et al. (2005)
Baranov et al. (2008)
Baranov et al. (2008), extrapolated
MT_CKD-4.0 (2022)
MT_CKD-4.0 ±10%
MT_CKD-4.0 ±20%
270 280 290 300 310 320 330
T / K

Figure 2.

2 × CO_2 radiative forcing
longwave feedback
surface feedback
atmospheric feedback
reference
continuum +10%
self cont. +10%
foreign cont. +10%
$\mathcal{F}_\nu$ / mW cm m^{-2}
λ_ν / mW cm m^{-2} K^{-1}
$\Delta\mathcal{F}_\nu$ / mW cm m^{-2}
$\Delta\lambda_\nu$ / mW cm m^{-2} K^{-1}
ν / cm^{-1}
T_s = 280 K
T_s = 300 K
T_s = 320 K

Figure 3.

2 × CO_2 radiative forcing $\mathcal{F}$

longwave feedback λ

climate sensitivity $\mathcal{S}$

total values

absolute changes

relative changes

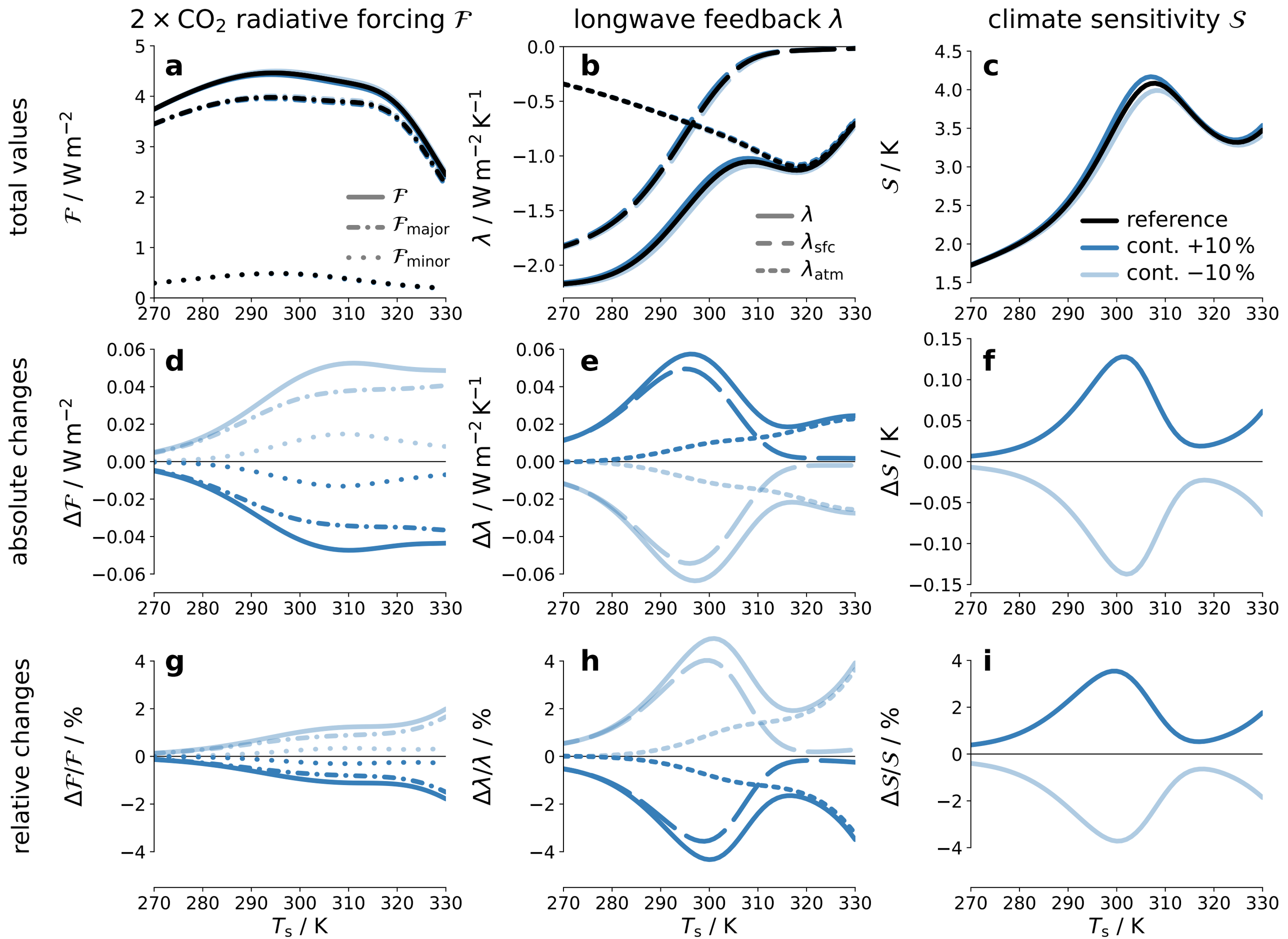

Figure 4.

a sketch of FIR

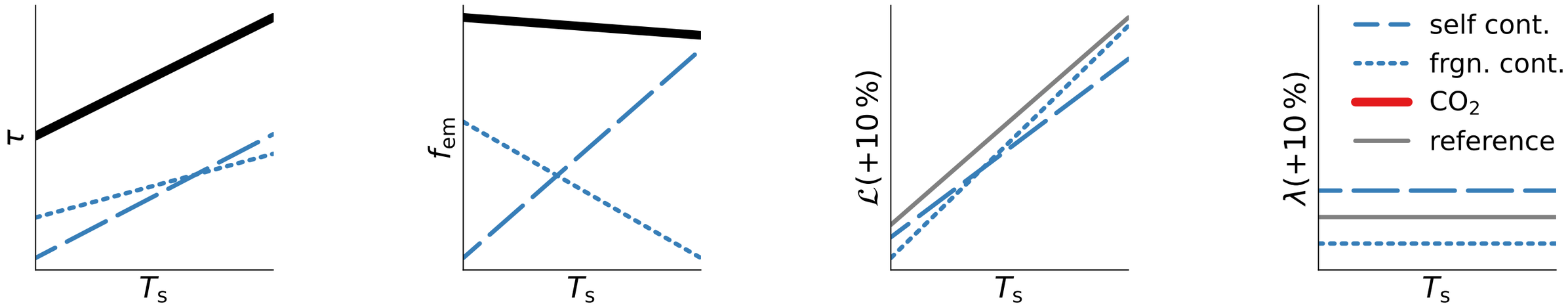

b FIR (200 cm^{-1} to 600 cm^{-1})

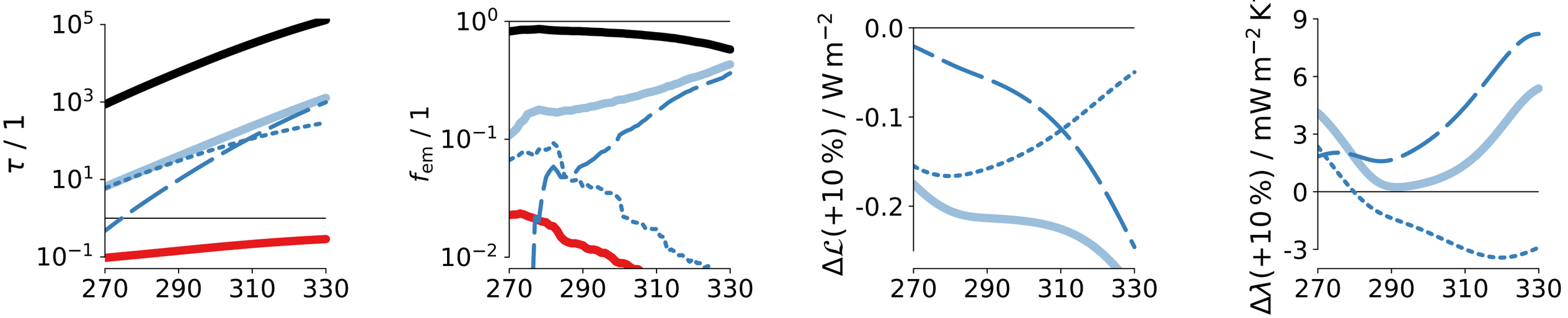

c CO_2 (600 cm^{-1} to 750 cm^{-1})

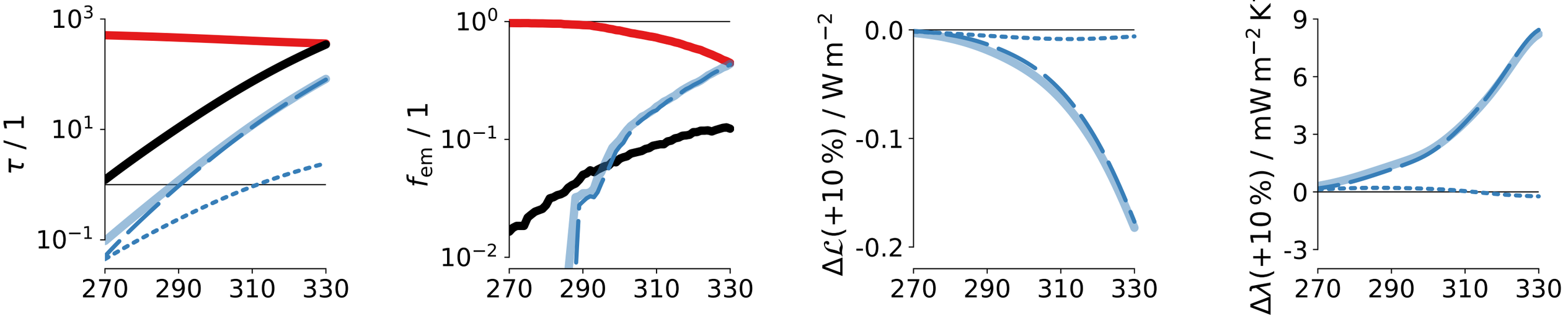

d window (750 cm^{-1} to 1250 cm^{-1})